JOURNAL OF CATALYSIS 142, 437–447 (1993)

Cu–Ru/MgO Systems—Spectroscopic Evidence of the Formation of Bimetallic Particles: CO Adsorption and CO–O_2 Interaction

G. GHIOTTI,*,[1] F. BOCCUZZI,* A. CHIORINO,* S. GALVAGNO,† AND C. CRISAFULLI‡

*Dipartimento di Chimica Inorganica, Chimica Fisica e Chimica dei Materiali, Facoltà di Scienze M. F. N., Università di Torino, Via Pietro Giuria, 7 I-10125 Turin, Italy; †Istituto di Chimica Industriale, Universtà di Messina, Cas. Post. 29, I-98010 Sant'Agata di Messina, Italy; and ‡Dipartimento di Scienze Chimiche, Laboratorio di Petrolchimica, Università di Catania, Viale A. Doria 8, I-95125 Catania, Italy

Received June 24, 1992; revised March 5, 1993

Ru/MgO, Cu/MgO, and Ru–Cu/MgO systems were characterized by FT-IR spectroscopy of adsorbed CO. The systems studied contained a total amount of metal of about 2 wt%: RCM100, RCM083, RCM070, RCM046, RCM034, and RCM000, with Ru/(Cu + Ru) atomic ratios 1, 0.83, 0.70, 0.46, 0.34, and 0.00, respectively. A comparison was made between the spectroscopic results and the catalytic properties in propane hydrogenolysis. On the Ru/MgO (RCM100) system CO originated an asymmetric band centered at 2038 cm^{-1}, shifting to lower frequency upon evacuation, in the spectral range of CO linearly adsorbed on (0001) faces. On Cu/MgO (RCM000) CO revealed the presence of two sites on which CO is adsorbed linearly giving bands at 2078 and 2060 cm^{-1}. On RCM083 catalyst large islands of uncovered Ru coexisted with areas of Ru heavily decorated by Cu, as revealed by the presence, upon CO adsorption, of a band at $\approx$2040 cm^{-1} and of a very broad band at $\bar{\nu} < 2000$ cm^{-1}. On RCM070 catalyst only areas of Ru heavily decorated by Cu were present, while on RCM046 and RCM034 samples large islands of uncovered Ru coexisted with areas of Ru heavily decorated by Cu, despite the increase in the Cu content. On the four bimetallic catalysts a variety of Cu(0) sites were revealed, bonding CO linearly (sharp CO stretching bands in the 2140–2098 cm^{-1} region), belonging to different Cu aggregates adsorbed on Ru microcrystals. These results are consistent with those obtained by catalytic measurements: the minimum catalytic activity and the maximum selectivity in ethane formation are found for the RCM070 sample, which shows only surface Ru(0) heavily decorated by Cu, as expected.

INTRODUCTION

During the recent past, bimetallic systems not forming bulk alloys have gained considerable attention. The Cu–Ru systems have been extensively studied, mainly as unsupported (*1–13*) or SiO_2 supported systems (*14–22*). All this work has shown that Cu interacts with Ru in a way similar to chemisorption, with Cu spread on the Ru-metal particles. The effect on Cu–Ru interaction of a wide variety of silica supports has been also investigated using H_2 chemisorption and several reactions of varying structure sensitivity (*20–22*). Recently some of us have shown through TPR (temperature programmed reduction) studies that the degree of Cu–Ru interaction, as well as the stability of bimetallic particles, is strongly dependent on the oxidic support used (*23*). In order to obtain more information on the influence of the support on the chemical properties of this bimetallic system, some of us studied propane hydrogenolysis on a series of pure Ru, pure Cu, and Ru–Cu catalysts supported on SiO_2, Al_2O_3, and MgO (*24*). Cu is known to be inactive in this reaction. On SiO_2 the hydrogenolysis activity of Ru decreased continuously by addition of copper over the entire range of composition. On Al_2O_3 and MgO it was found that on an increase in the amount of copper the catalytic activity initially decreased, reaching a minimum at Ru/(Ru + Cu) atomic ratios of $\approx$0.40 and $\approx$0.70 for Al_2O_3 and MgO, respectively; it then increased for higher Cu content. For each support, the less active samples were also

[1] To whom correspondence should be addressed.

0021-9517/93 $5.00

found to be the most selective towards ethane formation. The decreased catalytic activity has been attributed to the formation of Ru–Cu particles. The formation and composition of bimetallic particles have been related to the stages of formation and growth of the metal crystallites, but no catalyst characterization giving direct evidence of different degrees of interaction has been simultaneously done.

So far the study of the vibrations of the adsorbed molecules has been one of the most important tools employed in the surface characterization, and CO has been the most commonly used molecular probe for both mono- and bimetallic systems. However, for Ru–Cu supported systems, only IR studies on silica supported systems (*17–19*) have been carried out. The most recent paper of Liu *et al.* (*19*), concerning a large range of Ru/(Ru + Cu) atomic ratios has proved the formation of bimetallic particles: the increased CO stretching frequencies for the Cu–CO species and the lowered frequency for the Ru–CO species have been interpreted as a proof of Cu–Ru electronic interaction and attributed to a charge transfer from the Cu to the Ru, as expected (*13*). Furthermore the paper showed that the extent to which Ru is covered by Cu increases on increasing the amount of Cu, as hypothesized by some of us on the basis of the catalytic measurements made on systems prepared in the same way (*24*).

In the present paper the codispersion and interaction of Cu and Ru on MgO has been investigated for different Ru/(Ru + Cu) atomic ratios by the FT-IR study of adsorbed CO and CO/O_2 mixtures. The main scope is indeed to achieve direct evidence for the different degree of Cu–Ru interaction at different Ru/(Cu + Ru) atomic ratios and to do a comparison with the catalytic results. No FT-IR data are available, to our knowledge, for Cu–Ru/MgO systems.

EXPERIMENTAL

Materials. Commercial hydrated $RuCl_3$ and $Cu(NO_3)_2$ were used as precursor compounds. The support used (supplied as powder) was commercial MgO, Carlo Erba RPE-ACS, surface area 15 $m^2\ g^{-1}$.

Systems at different Cu–Ru ratios were prepared by impregnation of the support with aqueous solutions of $RuCl_3$ and $Cu(NO_3)_2$ having appropriate concentrations of metal. The amount of solution used was slightly greater than the pore volume. The salt(s) concentration in the solution was adjusted to yield a total (Cu + Ru) metal content of about 2 wt%. After impregnation the systems were dried at 393 K for about 24 h and reduced at 673 K for 1 h with a pure H_2 stream, in a microreactor.

Six samples with the following Cu and Ru wt% have been examined: Cu = 0, Ru = 2.09; Cu = 0.23, Ru = 1.82; Cu = 0.43, Ru = 1.61; Cu = 0.77, Ru = 1.03; Cu = 0.87, Ru = 0.70; and Cu = 2.0, Ru = 0. For the six catalysts the Ru/(Cu + Ru) atomic ratios are 1.00, 0.83, 0.70, 0.46, 0.34, and 0.00, respectively. On the basis of these ratios we named the six different samples RCM100, RCM083, RCM070, RCM046, RCM034, and RCM000, respectively.

Procedures. The powdered samples were pelleted (using a pressure of 20×10^3 kg/cm^{-2}) in self-supporting discs of ≈25 mg/cm^2 and ≈0.1 mm thick. Pellets were evacuated up to 673 K, reduced in pure H_2 for 1 h at 673 K, again evacuated at 673 K, and cooled to room temperature (RT) in an IR cell allowing thermal treatments in vacuum or in a controlled atmosphere. Then CO was admitted at increasing pressures to obtain the maximum coverage at RT (40–80 mbar). Subsequent evacuations were performed at RT or at higher temperature and CO was readmitted. To study the $CO–O_2$ coadsorption, the IR cell containing the sample in equilibrium with CO at the saturation pressure was allowed to face pure oxygen at a pressure of ≈30 mbar contained in a volume three times greater than that of the IR cell, and the gases were left to mix in contact with the sample overnight. The final partial pressures were $p_{CO} \approx 1–2$ mbar, $p_{O_2} \approx 20$ mbar. Finally the partial

pressure of CO was increased to 40 mbar, to obtain the saturation in CO of the oxidized surface. This oxidation procedure was chosen to avoid a too fast copper reoxidation reaction that could develop a high local heat that could be the origin of undesired metal sintering. The samples after reoxidation at RT were submitted to a new reduction–evacuation–CO-adsorption cycle to test the stability of the bimetallic systems.

The IR spectra were run on a Perkin–Elmer 1760-X FT-IR spectrophotometer with a resolution of 2 cm^{-1}. Data are reported as difference spectra obtained by subtracting the spectrum of the sample recorded before the interaction with CO and $CO–O_2$ and are normalized to the same amount of catalyst per cm^2 (25 mgr/cm^2).

No spectrum of adsorbed carbonyl species (2250–1750 cm^{-1}) has been revealed after contacting pure MgO, pretreated as previously described, with CO at RT. As a consequence all bands in the 2250–1750 cm^{-1} after CO interaction were assigned to copper or ruthenium carbonyls.

RESULTS AND DISCUSSION

Before starting to examine and discuss the spectroscopic data it is important to review the catalytic results obtained for Cu–Ru/MgO samples. Catalytic activities for propane hydrogenolysis are reported in Fig. 1 for nine different Ru/(Cu + Ru) atomic ratios. The measure of the catalytic activity has been evaluated on the basis of the following mechanism:

$$C_3H_8 + H_2 \rightarrow C_2H_6 + CH_4 \quad (1)$$

$$C_3H_8 + 2\,H_2 \rightarrow 3CH_4. \quad (2)$$

V is the rate of the overall reaction, calculated by the expression $V = (FX)/W$, where F is the feed rate of propane, X is the fraction of consumed propane, and W is the weight of Ru contained in the catalyst charge. The catalytic activity initially decreases on addition of Cu, reaching a minimum for the RCM070 sample. On further

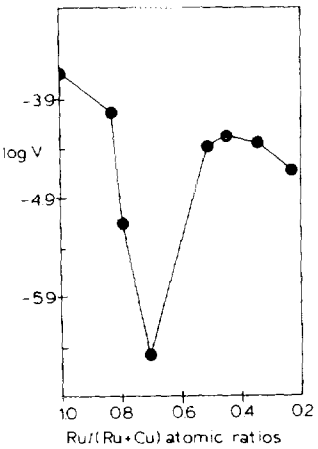

FIG. 1. Catalytic activity for hydrogenolysis of propane at 473 K over Ru–Cu/MgO samples vs. Ru/Ru + Cu ratios.

increase in the copper content (sample RCM055) it sensibly increases (even if to a value lower than for the pure Ru sample) and then remains practically constant for higher Cu contents.

Selectivity values measured at different temperatures (see Ref. (*24*) for more detailed information) showed that addition of Cu initially increases ethane selectivity, which reaches a maximum at 0.70 Ru/(Cu + Ru) ratio. At higher copper content the selectivity decreases (even if to a value higher than for the pure Ru sample).

To explain the lower activity and the higher ethane selectivity of the Ru–Cu systems it has been suggested (*24*) that the active sites are made by ensembles of n adjacent Ru atoms present at the surface and that the catalytic activity is related to the probability of finding such ensembles. The presence of inert copper on the surface would decrease the number of active ensembles. Reaction (1) has been reported (*25*) to require an ensemble of active atoms having a size smaller than that needed for reaction (2); therefore a dilution of Ru with inert copper would favor reaction (1), leading to an increase of selectivity. To explain the presence of the minimum in activity and a maximum in selectivity at 0.70 Ru/(Cu +

Ru) ratio, it has been suggested (*24*) that (i) up to this copper content nucleation centers of Ru are first formed on MgO support, on which copper is segregated; (ii) for higher copper content the probability that nucleation centers of Cu and Ru are formed simultaneously increases and monometallic particles can be formed. These suggestions will be tested in the following paragraphs.

CO adsorption on reduced monometallic systems. Figure 2a shows the spectra of CO adsorbed at RT on MgO samples supporting pure Ru (RCM100); Fig. 2b those on MgO supporting pure Cu (RCM000). Different curves concern different coverages. For the Ru/MgO (RCM100) system the main feature is a band at 2038 cm^{-1} at maximum CO coverage, shifting to lower frequency after evacuation. The spectral region is that of CO adsorbed on the (0001) face of a Ru macrocrystal (shifting from 2060 to 1980 cm^{-1} with CO coverage). The band is broader (*FWHM* = 45 cm^{-1}) in comparison to that for CO adsorbed on a macrocrystal (FHWM = 15 cm^{-1}), shows a tail on the low frequency side at maximum coverage. Furthermore, at low coverage, a variety of bands is observed: three components are evident at about 2010, 2000, and 1975 cm^{-1}. Broadening, asymmetry, and the presence of different bands can be caused by heterogeneity like that represented by CO located on different faces, on steps, corners, and/or at the border of the facets. However, these sites are not present in very large amounts; in fact the temperature for a complete CO desorption is 523 K, i.e., only 50 K higher than on the (0001) macroface. These results are consistent with data obtained from TEM (Transmission Electron Microscopy) analysis of the sample, showing Ru particles with diameter ranging from 10 to 120 Å (unpublished data). Similar results were found by Guglielminotti (*26*) on a Ru/MgO system prepared in the same way. The two small bands at 2080 and 2120 cm^{-1} are due to small fraction of unreduced Ru (*26–28*). No bands are detected in other spectral regions.

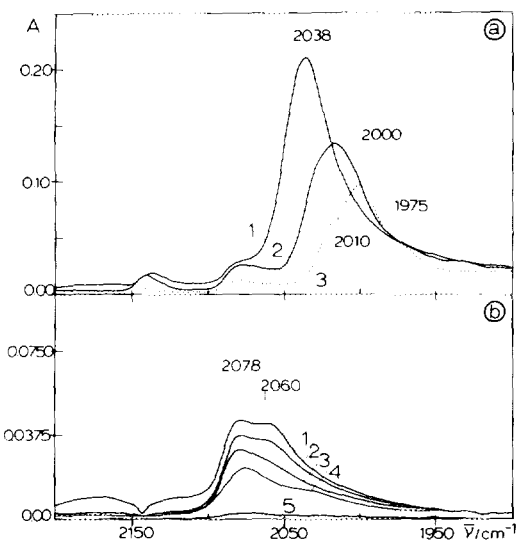

FIG. 2. (a) FT-IR spectra of CO adsorbed on RCM100 sample: curve 1, 40 mbar of CO; curve 2, after 15 min outgassing at RT; curve 3, after 10 min outgassing at 373 K. (b) FT-IR spectra of adsorbed CO on RCM000 sample: curve 1, 40 mbar of CO; curve 2, 9 mbar of CO; curve 3, 1 mbar of CO; curve 4, 0.3 mbar of CO; curve 5, after 10 sec outgassing at RT.

As far as the Cu/MgO (RCM000) system is concerned, CO is adsorbed at RT on the metal particles, as occurs on copper films and on copper particles supported on other oxides (*29–32*), the adsorption being highly pressure dependent. Spectra in the carbonyl region at maximum CO coverage show complex absorption with a pronounced tail at the low frequency side. Two bands are visible: one at 2078 cm^{-1}, another at 2062 cm^{-1} (more pressure dependent). They have both a FWHM of ca. 25–30 cm^{-1} (FWHM of bands of CO adsorbed on Cu macrofaces is 10 cm^{-1}). As the low frequency tail becomes relatively more important at lower coverages, it can be considered as due to CO adsorbed at the particle borderlines. For low-index (111), (110), and (100) planes of copper macrocrystals Pritchard *et al.* (*33*) recorded absorption maxima at 2075 to 2095 cm^{-1}, for CO adsorption at 77 K. The main maxima for the high-index stepped surfaces (211), (311), and

(755) were between 2095 and 2110 cm^{-1}. These single-crystal results point directly to the presence of low-index contributions to the microfacets of the Cu particle supported on MgO. However, while the peak at 2078 cm^{-1} has the same position as that for CO adsorbed on a (111) copper macroface, the component at 2062 cm^{-1} falls at a frequency unusual both for macrofaces and for supported copper particles. Actually, supported copper particles usually show CO bands at $\bar{\nu} \geq 2075$ cm^{-1}. However, a band at 2050 cm^{-1} near to the one at 2078 cm^{-1} has previously been observed on Cu/MgO by Davydov (*34*).

CO adsorption on Ru–Cu/MgO reduced systems. Figures 3a, 3b, 4a, and 4b show the results obtained for the samples RCM083, RCM070, RCM046, and RCM034, respectively. Different curves relate to different CO coverages.

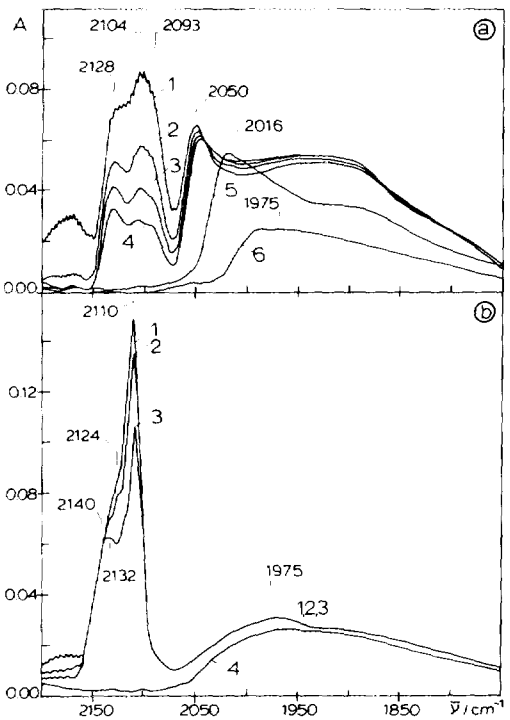

FIG. 3. (a) FT-IR spectra of CO adsorbed on RCM083 sample: curve 1, 70 mbar of CO; curve 2, 13 mbar of CO; curve 3, 4 mbar of CO; curve 4, 1 mbar of CO; curve 5, after 1 h outgassing at RT; curve 6, after 30 min outgassing at 373 K. (b) FT-IR spectra of CO adsorbed on RCM070 sample: curve 1, 40 mbar of CO; curve 2, 20 mbar of CO; curve 3, 5 mbar of CO; curve 4, after 15 min outgassing at RT.

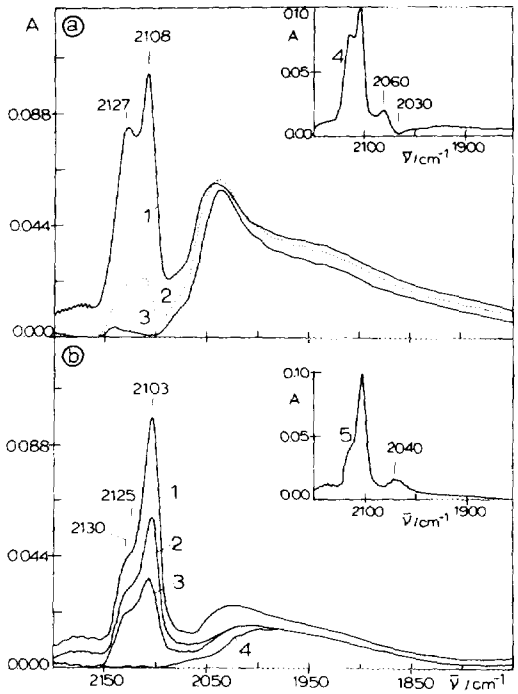

FIG. 4. (a) FT-IR spectra of CO adsorbed on RCM046 sample: curve 1, 40 mbar of CO; curve 2, 8 mbar of CO; curve 3, after 1 min outgassing at RT; cruve 4, difference between curve 1 and curve 3. (b) FT-IR spectra of CO adsorbed on RCM034 sample: curve 1, 40 mbar of CO; curve 2, 20 mbar of CO; curve 3, 5 mbar of CO; curve 4, after 5 min outgassing at RT; curve 5, difference between curve 1 and curve 4.

In the spectrum of CO adsorbed on RCM083 catalyst (see Fig. 3a) no bands at 2078 and 2060 cm^{-1} due to CO on pure copper particles are visible; a variety of new peaks are displayed at 2093, 2104, and 2128 cm^{-1} with FWHM < 20 cm^{-1}, all unstable under brief evacuation (1 min) at RT. Simultaneously the spectrum of CO adsorbed on Ru has been extensively perturbed: a band, characteristic of CO adsorbed on highly ordered Ru(0) areas, at about 2050 cm^{-1}, shifting to lower frequency by evacuation, is still present, but it is accompanied by a very broad absorption (FWHM $\approx$ 150–

200 cm^{-1}) with a large maximum at $\bar{\nu} < 2000$ cm^{-1}, partially unstable under 15 min of evacuation at RT and partially showing a higher stability.

Looking now at the RCM070 sample (Figure 3b), no bands due to CO on pure copper particles appear; four peaks at 2110, 2124, 2132, and 2140 cm^{-1} are present and are highly pressure dependent. Simultaneously the spectrum of CO adsorbed on extended ordered Ru regions is completely lacking. Only a very broad band (FWHM = 150–200 cm^{-1}) with maximum at $\approx$1970 cm^{-1} and stable under 15 min evacuation at RT is now present.

We assign the sharp peaks in the region 2140–2093 cm^{-1} to CO adsorbed on different Cu(0) sites, even if the assignment is not straightforward and requires a more detailed analysis. While peaks at 2093, 2104, and 2110 cm^{-1} are in the range of CO adsorbed on high index Cu(0) macrofaces, the 2124, 2128, 2132, and 2140 cm^{-1} frequencies are unusually high for CO adsorbed on Cu(0), both unsupported and supported on various oxides, and are positions characteristic of CO adsorbed on Cu(I) sites (*30, 32, 34*). However, the conditions of reduction used were strong enough to warrant complete copper reduction on Cu/MgO systems. Furthermore, the CO lability to the evacuation is that of CO adsorbed on Cu(0) sites. Looking at the IR data regarding CO adsorbed on Cu–Ru/SiO_2 systems (*17–19*), the C–O stretching frequencies of the Cu–CO carbonyls are shifted to higher values as compared to pure silica-supported Cu. These high frequencies are considered consistent with a positive polarization of the copper when supported on Ru, the higher polarization being, the lower is the copper content. However, on silica supported systems the phenomenon is slightly different as compared to that observed on our samples. Silica supported systems with different copper contents show, actually, only one C–O stretching band shifting from 2144 cm^{-1}, for material having low copper content, to 2123 cm^{-1}, for material with high copper content (*19*). On our samples a variety of bands is simultaneously present. Data from the literature (*11*) regarding a FT-IRAS study of CO adsorbed on Cu evaporated in different amounts and conditions on Ru(0001) macrofaces give a more important suggestion for our assignments. Copper films evaporated at 85 K on the Ru(0001) face exhibit a variety of adsorption sites when CO is used as probe molecule: small copper clusters of 1–4 atoms show C–O stretching frequencies in the range 2138–2123 cm^{-1}, two-dimensional aggregates show C–O stretching frequencies in the range 2120–2110 cm^{-1}, and three-dimensional aggregates show frequencies at about 2098 cm^{-1}. The range of C–O frequencies displayed is clearly that shown by our spectra, and allows us to hypothesize that the different peaks we saw are due to CO adsorbed on different aggregates of Cu(0) atoms, grown on the Ru particles. Different Ru crystallites may support Cu clusters with different sizes or Cu layers less or more extended, following the relative local concentration of Ru and Cu precursors. As no Cu(0)–CO species present on Cu/MgO system are detectable on the two examined samples we can conclude that in this range of content the copper does not segregate in monometallic particles.

Another problem is the nature of the sites related to the broad band at $\bar{\nu} < 2000$ cm^{-1}. Frequencies so low are indicative of very small Ru(0) clusters: a value of 2004 cm^{-1} was in fact calculated for a hexagonal CO island of 10 Å diameter on Ru(0001) face (*35*). The broadness and the asymmetry of this band (it shows a tail extending down to 1750 cm^{-1}) could be due to a high heterogeneity of species not only for a disordered situation (very small clean Ru areas of different sizes) but also for the formation of bridged carbonyls, the CO being coordinated to Ru–Ru or Ru–Cu sites. SSIMS studies of CO adsorption on Cu/Ru(0001) surfaces have demonstrated that Cu–Ru bridged CO and Ru–Ru bridged CO are likely surface species (*8, 36*). We remark

that Ru bridged carbonyls are not usual in either homogeneous or heterogeneous phase complexes. However, electron transfer from Cu to Ru in bimetallic particles could favor the stability of Ru bridged carbonyl species. In conclusion, we assign the broad absorption at $\bar{\nu} < 2000$ cm^{-1} to CO adsorbed on Ru(0) areas heavily decorated by copper.

On RCM046 reduced sample the CO spectrum (Fig. 4a) shows bands at 2127 and 2108 cm^{-1}, unstable under evacuation at RT, already assigned to CO adsorbed on different copper aggregates supported on Ru. As far as the use of CO as a probe of the Ru surface state is concerned, there is a band at about 2040 cm^{-1} with features characteristic of highly ordered surface Ru areas and a very broad band at about 1975 cm^{-1} already assigned to Ru areas heavily covered by copper. We may conclude that, despite the further increase in the copper content, large surface areas of Ru are not covered by Cu. It is difficult to state if small amounts of Cu segregate as monometallic particles. Surely the band at 2078 cm^{-1} is not present. A small positive peak at 2060 cm^{-1} and a small negative peak at 2030 cm^{-1} are visible in the difference between spectra before and after evacuation at RT (see Fig. 4a, curve 4). The 2060 cm^{-1} frequency corresponds to the other CO stretching vibration detected on the Cu/MgO sample and so could be assigned to CO adsorbed on small amounts of copper particles supported on MgO. However, the simultaneous presence of a negative peak at 2030 cm^{-1} in the same difference spectrum could be also interpreted as an effect of erosion and a shift to lower frequency of the band at 2040 cm^{-1} with evacuation.

Passing now to the RCM034 sample (the richest one in copper we examined by FT-IR spectroscopy) our expectation, on the basis of the catalytic data, was that a major amount of Cu would segregate as monometallic particles. This is not the case. The spectrum of adsorbed CO (see Fig. 4b) reveals the presence of (i) three sharp bands at 2130, 2125, and 2103 cm^{-1}, with the same features of the bands previously assigned to CO on different copper aggregates supported on Ru; (ii) a very broad absorption at lower frequencies with a tail extending to 1750 cm^{-1}, due to the superposition of a small absorption at 2040 cm^{-1} with FWHM $\approx$ 50 cm^{-1}, unstable under evacuation at RT (see Fig. 4b, curve 5) and of a very broad absorption with maximum at 2000–1980 cm^{-1}, which has the features previously assigned to CO adsorbed on Ru regions heavily decorated by Cu. The small band at 2040 cm^{-1} shows features typical of surface Ru carbonyls on extended islands of uncovered Ru(0). As no bands assigned to CO adsorbed on pure Cu particles are evident, no pure copper particles are present on this catalyst. As both islands of uncovered Ru(0) and heavily decorated Ru(0) regions are present, we imagine the following situation: first some copper segregates as pure particles, then they are completely covered by Ru layers, then Ru remains partially uncovered and is partially heavily decorated by other Cu atoms.

O_2 interaction with preadsorbed CO. Figure 5a shows the results obtained on the Ru/MgO sample. Ru(0) is only partially oxidized as revealed by the persistence of a band at 2040 cm^{-1}. Two new bands increase at 2138 and 2080 cm^{-1} that are stable under evacuation at room temperature. Minor features are shoulders at $\approx$2066 and 2000 cm^{-1}. The spectral characteristics (positions, integrate intensity ratio, FWHM) and stability under evacuation of the two main bands (2138, 2080 cm^{-1}) are the same as those of two bands previously found by CO adsorption on Ru/SiO_2 systems oxidized at RT, assigned to Ru(δ^+)$(CO)_3$ species (*27*). Bands with similar features have also been found on Ru/ZnO (*37*) and Ru/Al_2O_3 (*38*, *39*) systems by decomposition of $Ru_3(CO)_{12}$ and assigned to surface di-/tricarbonyl Ru(δ^+)$(CO)_{2,3}$ species, with δ near 3. Shoulders at about 2066 and 2000 cm^{-1} are very near in frequency to two bands at 2070–2005 cm^{-1} found on Ru/Al_2O_3 systems and

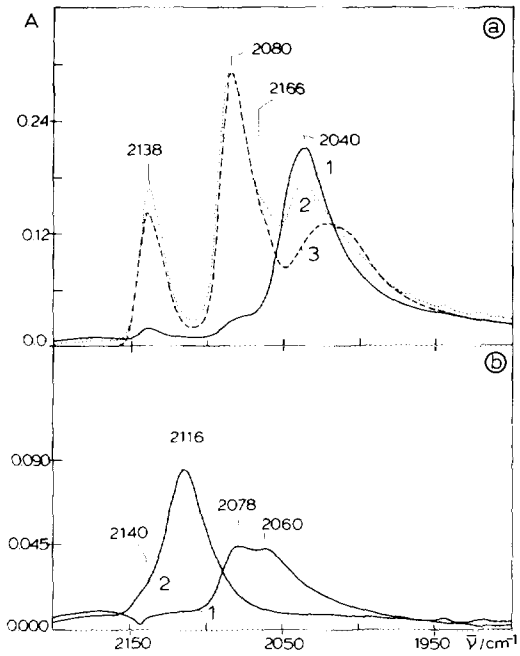

FIG. 5. (a) FT-IR spectra of O_2 interaction with CO preadsorbed on RCM100 sample: curve 1, the same as curve 1 of Fig. 2a; curve 2, after interaction with O_2 (as described in Experimental); curve 3, after 15 min outgassing at RT. (b) FT-IR spectra of O_2 interaction with CO preadsorbed on RCM000 sample: curve 1, the same as curve 1 of Fig. 2b; curve 2, after interaction with O_2 (as described in Experimental).

assigned to Ru $(\delta^+)(CO)_{2,3}$ surface species with δ near 2 (*38*, *39*). Very weak bands appear in the carbonate-like species region (1750–800 cm^{-1}, not reported in the figure), testifying that very small amounts of CO are oxidized to CO_2, and subsequently adsorbed on the MgO matrix.

On the Cu/MgO sample (see Fig. 5b) the bands of Cu(0)CO species are destroyed, giving a new band at 2116 cm^{-1} (FWHM ≈ 30 cm^{-1}) with a very small shoulder at ≈2140 cm^{-1}, both of which are unstable under prolonged evacuation (30 min) at RT. Owing to the mild oxidation condition used, a surface film of Cu_2O is formed (*31*), and we assign the 2116 cm^{-1} band to CO adsorbed on Cu(I) ions of the oxidized copper particles and the 2140 cm^{-1} band to CO adsorbed on oxidized copper atoms at the particle borderlines. Simultaneously large amounts of carbonate species are formed (not reported in figure).

On the four Cu–Ru/MgO systems, interaction with oxygen gives spectra very similar (see Figs. 6 and 7) in number and position of bands; however, some differences have to be noted. On samples RCM083 and RCM046, i.e., those showing the presence of large areas of ordered Ru(0), a fraction of Ru(0) is not oxidized, as revealed by the persistence, after oxidation, of a band at ≈2040 cm^{-1} partially unstable at RT (see Figs. 6a and 7a). Common features in the spectra of all samples are the increase of absorptions at 2126 cm^{-1}, 2078–2080 cm^{-1} and 2005 cm^{-1}. The absorption at 2126 cm^{-1} is indeed the sum of two main components, one at about 2124–2117 cm^{-1} unstable after prolonged evacuation (30 min) at RT, and

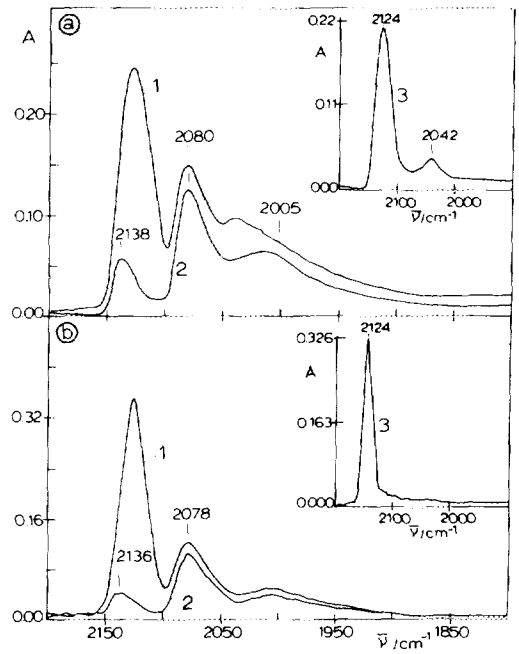

FIG. 6. FT-IR spectra of O_2 interaction with preadsorbed CO. (a) RCM083 sample: curve 1, after interaction of O_2 with preadsorbed CO as described in Experimental; curve 2, after 30 min outgassing at RT; curve 3, difference between curve 1 and curve 2. (b) RCM070 sample: curve 1, after interaction of O_2 with preadsorbed CO as described in Experimental; curve 2, after 30 min outgassing at RT; curve 3, difference between curve 1 and curve 2.

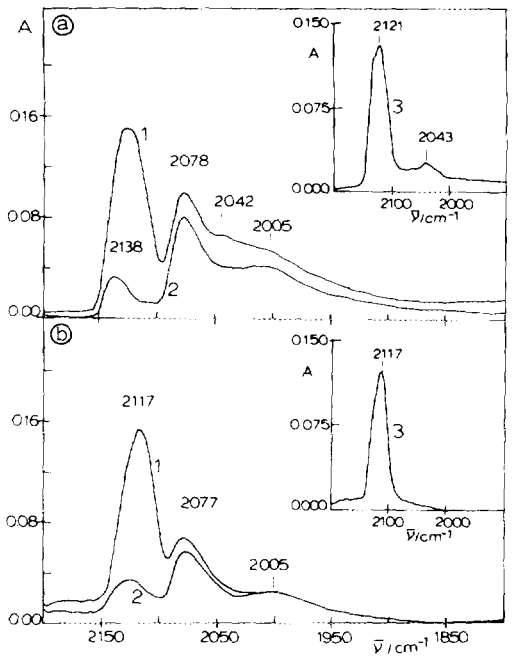

FIG. 7. FT-IR spectra of O_2 interaction with preadsorbed CO. (a) RCM046 sample: curve 1, after interaction of O_2 with preadsorbed CO as described in Experimental; curve 2, after 30 min outgassing at RT; curve 3, difference between curve 1 and curve 2. (b) RCM034 sample: curve 1, after interaction of O_2 with preadsorbed CO as described in Experimental; curve 2, after 30 min outgassing at RT; curve 3, difference between curve 1 and curve 2.

one stable under evacuation at about 2138–2125 cm^{-1}. The same stability under evacuation is shown by the bands at 2078–2080 and 2005 cm^{-1}.

The band at 2124–2117 has a frequency very near, and a stability under evacuation very similar to that observed by oxidation of pure copper particles: we assign it to CO adsorbed on oxidized copper. Bands at 2138–2125 and 2078–2080 cm^{-1} can be assigned to $Ru(\delta^+)(CO)_{2,3}$ with δ near 3. The band at 2078–2080 cm^{-1} actually shows a tail at lower frequency. It seems reasonable that also on these samples the band at 2078–2080 cm^{-1} is the superposition of two components, one at 2080 correlated to the 2138 cm^{-1} one, and another at 2072–2070 (responsible for the tail) associated to the band at 2005 cm^{-1} assignable at $Ru(\delta^+)(CO)_{2,3}$ with δ near 2.

The presence of Ru oxidation products indicates that on all bimetallic systems Ru atoms are present at the surface, as well as on the RCM070 sample on which the "classic" spectrum of Ru carbonyls ($\bar{\nu} \approx 2040$ cm^{-1}, shifting to lower frequency at low coverage) is absent. This is a further confirmation that the very broad band at 1975 cm^{-1} has been correctly assigned to Ru-carbonyls.

The amount of surface copper. The integrated intensity of the band at 2117–2124 cm^{-1}, assigned to Cu(I)CO species, is highly affected by the copper content and we have used it as a measure of the amount of oxidized copper exposed at the surface of our samples. To easily compare the different samples, we normalized the integrated intensities obtained for each sample to the same amount of copper, 0.43 mg/cm^2, i.e., the amount present in the RCM000 sample. The results are shown in Fig. 8 as open circles. In the same figure we have shown the integrated intensities (nor-

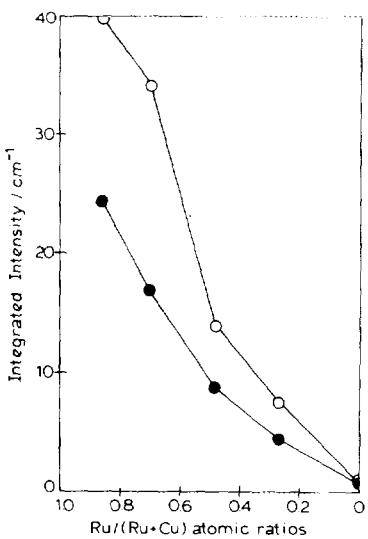

FIG. 8. Integrated intensities (normalized to 0.43 mg/cm^2 of copper) vs. Ru/Ru + Cu ratios of the bands related to CO adsorbed on reduced copper, solid circles; and of the bands related to CO adsorbed on oxidized copper, open circles.

malized to the same amount of copper) of the bands related to CO adsorbed on reduced copper as solid circles. To be clear, each solid circle represents the overall integrated intensity of the group of bands in the 2140–2093 cm^{-1} region. We have used this overall integrated intensity as a measure of the amount of surface Cu(0). This is a very coarse measure, and corresponds to the assumption that the extinction coefficients of the different Cu(0)CO species are the same. We can see a continuous increase in the integrated intensities related to the surface reduced copper with decreasing copper content; the same trend is also shown by the integrated intensities related to oxidized copper. These results are in good agreement with the other features of the spectra of CO adsorbed on reduced systems, indicating that for all examined bimetallic systems the surface copper is present as clusters or islands supported on Ru surface, even for the RCM046 and RCM034 samples. Obviously for these two systems, if our hypothesis sounds well, some copper is completely masked by Ru, but the exposed Cu has a surface area higher than if the total amount of copper segregated as pure copper particles. For the other systems, RCM070 and RCM083, all copper is reasonably dispersed on Ru. Therefore we can conclude that the lower the copper content is, the higher is the amount of copper exposed on the surface both in reduced or oxidized form, as revealed by the behaviour of the integrated intensities of the bands due to the carbonyl species reported in Fig. 8. Furthermore, the ratio between integrated intensities related to oxidized and reduced surface copper shows a value of ≈ 1.2 for the RCM000 sample, and higher values for the bimetallic systems: ≈ 1.6 for the RCM034 and RCM046 samples, ≈ 2 for the RCM070 sample, and ≈ 1.7 for the RCM083 sample. This is consistent with the fact that surface copper of pure metal particles is on flat microfacets, while copper supported on Ru presents roughness and so is easily oxidized.

CONCLUSIONS

On RCM083 catalyst large islands of uncovered Ru surface coexist with areas of Ru surface heavily decorated by copper. On RCM070 catalyst only areas of Ru surface heavily decorated by copper were present. On RCM046 and RCM034 catalysts large islands of uncovered Ru surface coexisting with areas of Ru surface heavily decorated by copper are again present, despite the increase in the copper content. The FT-IR results are qualitatively consistent with results obtained by catalytic measurements. The minimum catalytic activity and the maximum selectivity in ethane formation are found for sample RCM070, which shows only surface Ru(0) heavily decorated by copper. The hypothesis that, starting from Ru/(Ru + Cu) ratios lower than 0.70, pure Cu(0) and Ru(0) can originate simultaneously is only indirectly demonstrated. In fact, while the presence of pure Ru(0) particles is consistent with our IR analysis, in contrast no evidence of pure Cu(0) particles was found. In our opinion FT-IR data are consistent with the formation, starting from ratios <0.70, of particles with a nucleus of copper covered by Ru layers and then decorated by more copper. Obviously such a final situation requires an initial one where copper pure particles first segregate and then are completely recovered by Ru. The coverage with Ru of a Ib-group metal has already been put in evidence in the Ru–Au/MgO system and has been attributed to a strong interaction of the noble metal with the MgO support (*40*).

ACKNOWLEDGMENT

This work was partially supported by a financial contribution from the Progetto Finalizzato Chimica Fine II (CNR).

REFERENCES

1. Sinfelt, J. H., Lam, Y. M., Cusumano, J. A., and Barnett, A. E., *J. Catal.* **42,** 227 (1976).
2. Christmann, K., Ertl, G., and Shimizu, H., *J. Catal.* **61,** 397 (1980).
3. Vickerman, J. C., Christmann, K., and Ertl, G., *Surf. Sci.* **71,** 175 (1981).

4. Shi, S. K., Lee, H. I., and White, J. M., *Surf. Sci.* **102,** 56 (1981).
5. Vickerman, J. C., and Christmann, K., *Surf. Sci.* **120,** 1 (1982).
6. Vickerman, J. C., Christmann, K., and Ertl, G., *Surf. Sci.* **134,** 367 (1983).
7. Brown, A., and Vickerman, J. C., *Surf. Sci.* **140,** 261 (1984).
8. Brown, A., van der Berg, J. A., and Vickerman, J. C., *in* "Proceedings, 8th International Congress on Catalysis, Berlin, 1984," Vol. IV, p. 35. Dechema, Frankfurt-am-Main, 1984.
9. Paul, J., and Hoffmann, F. M., *Surf. Sci.* **172,** 151 (1986).
10. Rocker, G., Toshihara, H., Martin, R. M., and Metiu, H., *Surf. Sci.* **87,** 509 (1987).
11. Hoffmann, F. M., and Paul, J., *J. Chem. Phys.* **86,** 2990 (1987) (a), and **87,** 1857 (1987) (b).
12. Hoffmann, F. M., Rocker, G., Toshihara, H., Martin, R. M., and Metiu, H., *Surf. Sci.* **205,** 397 (1988).
13. Houston, J. E., Peden, C. H. F., Blair, D. S., and Goodman, D. W., *Surf. Sci.* **167,** 427 (1986).
14. Sinfelt, J. H., *J. Catal.* **29,** 308 (1973).
15. Bond, G. C., and Yide, X., *J. Mol. Catal.* **25,** 141 (1984).
16. Lai, S. Y., and Vickerman, J. C., *J. Catal.* **90,** 337 (1984).
17. Guo, X., Xin, Q., Li, Y., Jin, D., and Ying, P., *in* "Proceedings, 8th International Congress on Catalysis, Berlin, 1984," Vol. IV, p. 599. Dechema, Frankfurt-am-Main, 1984.
18. Hong, A. J., McHugh, B. J., Bonneviot, L., Resasco, D. E., Weber, R. S., and Haller, G. L., *in* "Proceedings, 9th International Congress on Catalysis, Calgary, 1988" (M. J. Phillips and M. Ternan, Eds.), Vol. 3, p. 1198. Chem. Institute of Canada, Ottawa, 1988.
19. Liu, R., Tesche, B., and Knözinger, H., *J. Catal.* **129,** 402 (1991).
20. Haller, G. L., Resasco, D. E., and Wang, J., *J. Catal.* **84,** 477 (1983).
21. Rouco, A. J., Haller, G. L., Oliver, J. A., and Kemball, C., *J. Catal.* **84,** 297 (1983).
22. Hong, A. J., Rouco, A. J., Resasco, D. E., and Haller, G. L., *J. Phys. Chem.* **91,** 2665 (1987).
23. Galvagno, S., Crisafulli, C., Maggiore, R., Giannetto, A., and Schwank, J., *J. Therm. Anal.* **32,** 471 (1987).
24. Crisafulli, C., Maggiore, R., Schembari, G., Sciré, S., and Galvagno, S., *J. Mol. Catal.* **50,** 67 (1989).
25. Dalmon, J. A., and Martin, G. A., *J. Catal.* **66,** 214 (1980).
26. Guglielminotti, E., *Langmuir* **2,** 812 (1986).
27. Schwank, J., Parravano, G., and Gruber, H. L., *J. Catal.* **61,** 19 (1980).
28. Yokomizo, G. H., Louis, C., and Bell, A. T., *J. Catal.* **120,** 1 (1989).
29. Toolemaar, F. J. C. M., van der Poort, G. J., Stoop, F., and Ponec, V., *J. Chim. Phys.* **78,** 927 (1981).
30. Kohler, M. A., Cant, N. W., Wainwright, M. S., and Trimm, D. I., *J. Catal.* **117,** 188 (1989).
31. Boccuzzi, F., Ghiotti, G., and Chiorino, A., *Surf. Sci.* **156,** 933 (1985).
32. Roberts, D. L., and Griffin, G. L., *J. Catal.* **110,** 117 (1988).
33. Pritchard, J., Catterick, T., and Gupta, R. K., *Surf. Sci.* **53,** 1 (1975).
34. Davydov, A., *Kinet. Katal.* **26,** 157 (1985).
35. Pfnür, H., Menzel, D., Hoffmann, F. M., Ortega A., and Bradshaw, A. M., *Surf. Sci.* **93,** 431 (198).
36. Sakakini, B., Swift, A. J., Vickerman, J. C., Harendt, C., and Christmann, K., *J. Chem. Soc. Faraday Trans. 1* **83,** 1975 (1987).
37. Guglielminotti, E., and Boccuzzi, F., *in* "Structure and Reactivity of Surfaces" (C. Morterra, A. Zecchina, and G. Costa, Eds.), Studies in Surface Science and Catalysis, Vol. 48, p. 437. Elsevier, Amsterdam, 1989.
38. Zecchina, A., Guglielminotti, E., Bossi, A., and Camia, M., *J. Catal.* **74,** 225 (1982).
39. Guglielminotti, E., Zecchina, A., Bossi, A., and Camia, M., *J. Catal.* **74,** 240 (1982).
40. Bassi, I. W., Garbassi, F., Vlaic, G., Marzi, A., Tauszik, G. R., Cocco, G., Galvagno, S., and Parravano, G., *J. Catal.* **64,** 405 (1980).